AAPS PharmSciTech (2023) 24:115
https://doi.org/10.1208/s12249-023-02571-2

RESEARCH ARTICLE

Advancements in Amorphous Solid Dispersions to Improve Bioavailability

Enhancement of Valsartan Oral Bioavailability by Preparing a Microwave-Irradiated Inclusion Complex with Sulfobutyl Ether *β*-Cyclodextrin Using a Central Composite Face Design for Optimising Process Parameters

Venkata Ramana Maddula[1,2] · **Rama Sekhara Reddy Dachuru**[3]

Received: 1 February 2023 / Accepted: 17 April 2023 / Published online: 9 May 2023

Abstract

The purpose of the study is to investigate the influence of sulfobutyl ether β-cyclodextrin (SBE_7-β-CD) on the bioavailability of valsartan. Phase solubility investigations showed an A_L type curve. The estimated apparent stability constant for valsartan SBE_7-β-CD is $427 \pm 0.32\ M^{-1}$. Inclusion complexes of valsartan SBE_7-β-CD in equal molar ratio were prepared by microwave irradiation technique. The process parameters were optimised with a central composite face design. Response surface graphs and contour plots showed how process factors affected drug content. The inclusion complexes prepared by optimising process variables are characterised. The DSC and X-ray diffraction confirm the formation of inclusion complexes and the drug's transition from a crystalline to an amorphous state. FTIR suggests hydrogen bonding between valsartan and SBE_7-β-CD. SEM showed changes in drug morphology and shape. The dissolution rate of the prepared SBE_7-β-CD complex using microwave irradiation was 2.85 times that of pure valsartan. The inclusion complex was formulated into tablet dosage forms F_1 to F_4. Furthermore, oral bioavailability studies in rats with tablet formulation F_3 were carried out and compared to the marketed Diovan® tablet as a reference standard. The F_3 tablet formulation exhibited significantly higher values of $AUC_{0\text{-}\infty}$ and C_{max} than the reference. Finally, the microwave-irradiated valsartan SBE_7-β-CD inclusion complex converted into tablet dosage form may be a promising approach to increasing valsartan oral bioavailability.

Keywords Microwave-irradiated inclusion complexes · Modified β-cyclodextrin · Response surface methodology · SBE_7-β-CD · Valsartan

Introduction

Valsartan is a drug used for hypertension that works by blocking the angiotensin II type 1 receptor [1, 2]. The Biopharmaceutical Classification System (BCS) categorises valsatan as a molecule of class II, which is water-insoluble and highly permeable [3–5]. Due to its limited water solubility, valsartan has a low bioavailability [6], ranging from 23 to 39% [7]. Although several approaches for improving the physicochemical and biological characteristics of water-insoluble drugs have been developed, each has its own limitations [8]. Numerous strategies have been proposed in order to solve this issue. One of the more promising methods among them is the complexation of the drug with cyclodextrins. Oligosaccharides with varying glucopyranose rings are cyclodextrins.

Cyclodextrins have a lipophilic core and a hydrophilic shell, making them suitable for association complexes with lipophilic drugs [9]. The complexation of drugs with cyclodextrins using a variety of methodologies indicated the value

✉ Rama Sekhara Reddy Dachuru
mvr_pharma@vignan.ac.in; dachuru@gmail.com

Venkata Ramana Maddula
mvramanapharmacist@gmail.com

[1] Department of Pharmaceutical Sciences, Vignan's Foundation for Science, Technology & Research, Vadlamudi 522213, Andhra Pradesh, India

[2] Faculty of Pharmacy, Krishna University, Machilipatnam 521004, Andhra Pradesh, India

[3] Department of Chemistry, Krishna University, Machilipatnam 521004, Andhra Pradesh, India

of cyclodextrins in enhancing the solubility of pharmaceuticals [10]. Cyclodextrins improve the solubility of weakly water-soluble drug when complexed with them. However, nephrotoxicity hinders the use of cyclodextrins in pharmaceutical formulations. With the discovery of numerous chemically altered cyclodextrins, such as sulfobutyl ether cyclodextrin (SBE_7-β-CD), which have significantly lower toxicity, interest in the use of cyclodextrins has grown, particularly for increasing the dissolution, stability, and bioavailability of drugs that are poorly water-soluble [11]. Sulfobutyl ether β-cyclodextrin is a chemically modified β-CD that is a negatively charged cyclic hydrophilic oligosaccharide in aqueous media. At 25 °C, aqueous solubility is 70 g/100 ml, which exceeds β-CD. Furthermore, there is no nephrotoxicity, unlike β-CD [12]. Due to these benefits, SBE_7-β-CD may improve the physiochemical properties of weakly water-soluble compounds.

Cyclodextrin complexes are traditionally prepared using a variety of methods. Co-evaporation, spray drying, and freeze drying are examples of these techniques. All these procedures have key drawbacks, such as co-evaporation and spray drying require a substantial amount of organic solvent and often have a low yield [13], whereas freeze drying is time-consuming and produces hydroscopic products [14]. To avoid the drawbacks of existing complexation procedures, a novel technology such as microwave irradiation (MWI) is being explored. On the other hand, MWI will have fewer scale up issues [15]. In order to improve the bioavailability of valsartan, researchers have established various approaches using β-cyclodextrin, hydroxypropyl β-cyclodextrin, and methyl β-cyclodextrin, where there is no data reported using SBE_7-β-CD or the microwave irradiation method [16–18].

The objective of the study is to synthesise a cyclodextrin complex with optimised process parameters and determine the effect of SBE_7-β-CD on valsartan dissolution. This research also looked into the characterisation of a complex formed by valsartan and SBE_7-β-CD using an industrially viable microwave irradiation method. Finally, *in vivo* pharmacokinetic investigations have been conducted on the cyclodextrin complex compared with the pure drug.

Materials and Methods

Materials

Valsartan was obtained from Aurobindo Pharma Limited in Hyderabad as a free sample. SBE_7-β-CD was acquired from Shanghai-based Chembest Research Laboratories Limited. Every other substance, including solvents, was of analytical grade.

Phase Solubility Studies

Regarding valsartan and SBE_7-β-CD stochiometry, phase solubility studies are performed. Phase solubility measurements of SBE_7-β-CD and valsartan were performed using the Higuchi-Connors technique [19]. In separate conical flasks holding 10 ml of distilled water having increasing concentrations of SBE_7-β-CD starting from 0.5 to 5 mM, an excess of valsartan was added. After 24 h of shaking, the suspension was filtered through 0.45-µm filter paper, diluted as necessary, and analysed. According to the following equation, we were able to deduce the stability constant Ks using the phase solubility diagram.

$$Ks = \frac{slope}{So(1 - slope)}$$

where S_0 is the valsartan water solubility.

Estimation of Gibbs Free Energy

The ratio of the molar solubility of valsartan in carrier solution (Ss) and the molar solubility of the drug in solution (Sw) can be considered as a partitioning ratio. Therefore, the Gibbs free energy transfer (ΔG_{tr}°) from the solution to the carrier solution can be calculated as:

$$\Delta G_{tr}^{\circ} = -RT \ln(Ss/Sw)$$

where R = gas constant is 8.31 J/K/mol and T is temperature in Kelvin.

Preparation Inclusion Complexes

Preparation of Physical Mixture

Based on the preliminary phase solubility investigations, an equal molar ratio (1:1) mixture of valsartan and SBE_7-β-CD was produced. The physical mixture (PM) was made by simply combining correctly weighed quantities in a mortar for 2 min with a spatula [20].

Kneading Method

To prepare the equal-molar binary system via the kneading technique, weighed amounts of valsartan and SBE_7-β-CD were placed in a mortar and mixed for 20 min. The final mixture was kneaded for a further 45 min with a few drops of ethanol. The resultant paste was dried overnight in a vacuum desiccator. The dried

product was collected after passing through screen number 60 [21].

Microwave Irradiation Technique and Optimisation

Preliminary Trials In order to make inclusion compounds, it is crucial to understand the process variables. A physical mixture of valsartan (435.5 mg) and SBE_7-β-CD (2083 mg) in an equal molar ratio (1:1) with specified quantity of ethanol was subjected to microwave treatment in a microwave oven with a single magnetron emitter that operates at 2.45 GHz. On the instrument's Pyrex turntable, the sample was rotated to achieve consistent irradiation. The solvent quantity is kept constant in all conditions. The irradiated samples were washed with ethanol to remove the free drug stored in a desiccator [22–26].

Optimisation of Process Variables with Design of Experiments There were some preliminary tests done to find out the processing range of independent variables. The effect of processing parameters, i.e., power, reaction time, and amount of solvent, was examined using an experimental design and statistical analysis of the data. The process parameters were optimised using a central composite design, with α face centred [27]. Three independent variables were chosen, namely, microwave power of 200 to 600 W (X_1), reaction time of 10 to 120 s (X_2), amount of solvent of 1 to 3 ml (X_3), and percentage drug content (R_1) as a dependent variable. Each independent variable consisted of three levels, which were represented by the values − 1, 0, and + 1, respectively. The quadratic model proved statistically significant at $p < 0.05$ in the process optimisation data analysis. Stat Ease Design Expert 13 developed quadratic terms for the response variable in polynomial models utilising multiple linear regression analysis. The following polynomial equation gives a description of the influence [28]:

$$R_1 = \beta_0 + \beta_1 X_1 + \beta_2 X_2 + \beta_3 X_3 + \beta_{12} X_1 X_2 + \beta_{13} X_1 X_3 + \beta_{23} X_2 X_3 + \beta_{11} {X_1}^2 + \beta_{22} {X_2}^2 + \beta_{33} {X_3}^2$$

In the equation above, R_1 stands in for the dependent variable, i.e., percentage drug content. The value β_0 represents the intercept as well as the mean of twenty runs. The values β_1, β_2, β_3, β_{12}, β_{13}, β_{23}, β_{11}, β_{22}, and β_{33} represent the estimated variable coefficients X_1, X_2, X_3, X_1X_2, X_1X_3, X_2X_3, ${X_1}^2$, ${X_2}^2$, and ${X_3}^2$, respectively. The average effect of making one variable go from low to high is the main effect of X_1, X_2, and X_3. When two factors are changed at the same time, the interaction terms X_1X_2, X_1X_3, and X_2X_3 show how the parentage drug content varies. The data or model could be incorrect if the predicted and adjusted R^2 were less than 0.20. The coefficient was significant if $p < 0.05$. SNR determines precision. It compares the design point prediction range to the typical forecast error. Ratios over four suggest adequate model discrimination. One-way analysis of variance ($p < 0.05$) verifies model significance [29].

Model Validation and Optimisation Numerical optimisation is desirability-based, and graphical optimisation with the use of overlay graphs was used to review the developed mathematical model's optimisation potential in light of the central composite design, with α face centred. By imposing constraints on each factor and response, an optimal process was developed. The factors' optimal ranges were constrained to $200 \le X_1$ 600 W target 400 W, $10 \le X_2 \le 120$ s, and $1 \le X_3 \le 3$ ml, while response ranges were limited to $80 \le Y \le 98\%$. Estimated model accuracy is obtained by preparing inclusion complexes with three sets of conditions having the optimal combination of the factors recommended by the programme. The chosen optimised process variables were employed to prepare the inclusion complex to achieve a target value of 90% drug content. The percentage relative error was calculated by [28, 29]:

$$\%\ Error = \frac{\text{Experimental value} - \text{Predicted value}}{\text{Predicted value}} \text{X } 100$$

Analysis of Drug Content

In methanol, an inclusion complex containing 10 mg of valsartan was dissolved and filtered through a membrane filter. Utilising a UV–visible spectrophotometer at 250 nm, the quantity of valsartan in the filtrate was determined [30].

In Vitro Dissolution Rate

The dissolution rate of valsartan and valsartan SBE_7-β-CD inclusion complexes was evaluated in a pH 6.8 phosphate buffer. The dissolution tests were performed with a USP XXIII type 2 dissolution rate test apparatus at a temperature of 37 ± 0.5 °C and a paddle speed of 50 rpm for 30 min. Each basket containing 1000 ml of dissolution medium received an inclusion complex weight, which is equivalent to 40 mg of pure valsartan. At various time periods, a 5-ml aliquot was withdrawn and filtered using a 0.45-µm nylon disc filter. The filtered samples were suitably diluted if necessary and assayed spectrophotometrically by measuring absorbance at 250 nm. The dissolution experiment was conducted in sink conditions [31]. The dissolution of the prepared formulations and Diovan® was also tested using the same method. Further, the difference factor (f_1) is a measure of the relative inaccuracy, while the similarity factor (f_2) is a measure of the resemblance between two curves' dissolution. These parameters were determined for the optimal formulation and the formulation sold on the market [32].

Formulation of Inclusion Complex into Tablets

The inclusion complex of valsartan prepared by microwave irradiation technology (VSMWC 3) is compressed directly into tablets [33]. Inert components such as crospovidone, which served as a superdisintegrant; microcrystalline cellulose, which served as a directly compressible vehicle; colloidal silicon dioxide, which served as a glidant; and magnesium stearate, which served as a lubricant, were used to make the tablets. The percentage of crospovidone is varied from 2 to 5% in order to formulate the four distinct formulations, F_1 to F_4, mentioned in Table I. The components were weighed and combined proportionally. In a resealable plastic bag, the mixture was mixed for 20 min. Lastly, glidant and lubricant were added, and the mixture was mixed for 2 min. The precompression parameters of the resulting mixture for each formulation were analysed. The resulting homogenous mix was used to create the tablets by being directly compressed using a mini press compression machine equipped with a circular flat-faced punch 8 mm in diameter. The prepared formulations were evaluated for quality control tests.

Weight Variation Test

The weight variation test was carried out by individually weighing 20 tablets with an electronic digital balance. The average weight was then computed and compared to the weight of each tablet individually. The mean ± standard deviation (SD) was noted.

Friability

The friability of the tablets was determined by a tablet friability tester (Model FT 1020, Labindia). Six grammes of tablets were carefully weighed (W_1) and placed in the tablet friabilator's drum, which spins for four minutes at a speed of 25 revolutions per minute. Afterwards, the tablets were dusted and reweighed (W_2). The percentage weight loss was used to calculate the tablet friability using the following equation:

$$\text{Percentage friability} = \frac{W1 - W2}{W1} \times 100$$

Tablet friability < 1% was acceptable.

Drug Content

In a mortar, ten random tablets from each formulation were crushed finely. A magnetic stirrer was used to completely mix an amount of powder equal to the weight of one tablet into 500 ml of phosphate buffer pH 6.8. After filtering and appropriately diluting the solution with phosphate buffer pH 6.8, the drug concentration was evaluated by spectrophotometric analysis at a wavelength of 250 nm using a UV–Visible spectrophotometer. Each sample was examined three times.

Disintegration Test

The Labindia disintegration tester was used to calculate the disintegration time for six tablets from each batch. Each tablet was put into one of the basket's six tubes. Each tube has a disc added to it. The apparatus was run using 1000 ml of phosphate buffer solution (pH 6.8) maintained at 37 ± 0.5 °C. At a fixed rate of 30 cycles per minute, the basket assembly was lifted and lowered. The amount of time, in seconds, required for the tablets to completely dissolve, leaving no discernible mass inside the device was measured and recorded.

Fourier Transform Infrared Spectroscopy

The FTIR spectra were taken using a spectrophotometer (CARY 630 from Agilent Technologies, USA) using the KBr pellet method. The scans were taken at a scanning speed of 2 mm per second with a resolution of 4 cm^{-1}, scanning the range between 600 and 4000 cm^{-1}, while the device was operating in dry purge [34].

Thermal Analysis

Differential scanning calorimetry (DSC) analysis was performed by Exstar 7020, Hitachi HTG, Japan, utilising a 5 mg sample at 10 °C per minute from 40 to 300 °C. The reference was an empty aluminium pan. All studies employed 30 ml per minute of nitrogen purge gas [35].

Table I Formula for the preparation of valsartan tablets

Ingredient	F_1	F_2	F_3	F_4
VSMWC 3 complex equivalent to valsartan 40 mg	185 mg	185 mg	185 mg	185 mg
Crospovidone	6 mg (2%)	9 mg (3%)	12 mg(4%)	15 mg (4%)
Magnesium stearate	3 mg (1%)	3 mg (1%)	3 mg (1%)	3 mg (1%)
Colloidal silicon dioxide	3 mg (1%)	3 mg (1%)	3 mg (1%)	3 mg (1%)
Microcrystalline cellulose q.s to	300 mg	300 mg	300 mg	300 mg

Powder X-Ray Diffraction

A Rigaku Miniflex 600 X-ray diffractometer was used to examine the crystalline state of valsartan in prepared inclusion complexes. Cu Kα radiation at 40 kV and 15 mA was used as the X-ray source. The samples were analysed in continuous scan mode at 5 degrees per minute, with a scanning range 0–90 degrees.

Areas of crystalline (Ac) and amorphous (Aa) diffraction peaks were substituted in the following equation for determining the degree of crystallinity [36].

$$\text{Percentage Crystallinity} = \frac{\text{Area under the crystalline peaks (Ac)}}{\text{Area under all peaks (Ac + Aa)}} X\ 100$$

Scanning Electron Microscopy Studies

A scanning electron microscope (VEGA 3, TESCAN) examined the pure drug, physical mixture, and inclusion complex surfaces. The sputter coater, Cressington 108, USA, coated the samples with a very thin coating of gold, which makes them conductive to electricity. Photos were collected at 20 kV [37].

Bioanalytical Method for Estimating Valsartan in Rat Plasma

In this study, a sensitive high-performance liquid chromatography (HPLC) method was created and tested to measure the amount of valsartan in the blood. Waters Arc HPLC System, inertsil ods column (150 mm × 4.6 mm, 5 µm), mobile phase was acetonitrile: 20 mM potassium dihydrogen orthophosphate buffer pH 3 (adjusted with 50% orthophosphoric acid) at 65:35 v/v, 1 ml/min flow rate, run time 5 min and photodiode array detector (PDA) detector wavelength of 224 nm. Telmisartan was used as the internal standard. The peak area ratio of valsartan and the internal standard were used to estimate the concentrations. The US Food and Drug Administration (USFDA) requirements for bioanalytical technique validation were followed in the development and verification of the method [38]. Selectivity, linearity, ruggedness, recovery, and stability were all within the acceptable range set by the Food and Drug Administration.

Sample Preparation and Analysis

The plasma proteins were precipitated to extract valsartan from the plasma before the sample was injected. 0.2 ml of plasma was mixed with 0.5 ml of internal standard (IS) and 1.3 ml of acetonitrile solution and vortexed for 10 min, after which the sample was centrifuged for twenty minutes at 7500 rpm. Ten microliters of centrifuged supernatant was analysed.

In Vivo Pharmacokinetic Study

Twelve male Wistar rats weighing 200–250 g and 9–12 weeks old that had fasted for 12 h before to the experiment were used in the study. There were two groups of six rats each. The formulations were administered orally to each rat at a dose level of 10 mg/kg [39]. Group 1 receives a Diovan®, while group 2 receives a prepared tablet formulation F_3. Blood aliquots of 0.3 ml were taken from the retro orbital sinus of rats and kept in microfuge tubes with dipotassium ethylene diamine tetra acetic acid. The samples were taken at 0-, 0.25-, 0.5-, 0.75-, 1, 1.25-, 1.5-, 2-, 4-, 6-, 8-, 12-, 18-, and 24-h post-dose. After immediately centrifuging the sample at 7500 rpm for 20 min to separate the plasma, the plasma was then placed in a frozen state for storage. PK solver's basic non-compartmental analysis was used to determine pharmacokinetic variables such as the maximum plasma concentration (C_{max}), the time at which it occurs (T_{max}), and the area under the curve (AUC) for each rat [40]. The Institutional Animal Ethics Committee approved the protocol (Approval No. 05/IAEC/VPC/2022).

Results and Discussion

Phase Solubility Studies

The diagram for the phase solubility of valsartan with SBE_7-β-CD is shown in Fig. 1. The pure valsartan intrinsic solubility (S_0) was 0.125 mg/ml. Valsartan solubility rises linearly with SBE_7-β-CD concentration over the concentration range, revealing an A_L-type diagram. Therefore, inclusion complexes with an equal molar ratio (1:1) were prepared. The estimated Ks for valsartan SBE_7-β-CD inclusion complex was $427 \pm 0.32\ M^{-1}$. Thus, it can be said that valsartan makes more stable complexes with SBE_7-β-CD. This may be because it makes the hydrophobic cavity bigger without steric hindrance and makes it easier to fit into the cavity.

Estimation of Gibbs Free Energy

The ΔG_{tr}° values are becoming increasingly negative, indicating that valsartan undergoes spontaneous solubilisation. The ΔG_{tr}° value indicates that the ratios used were considered to be appropriate for the drug's solubilisation and

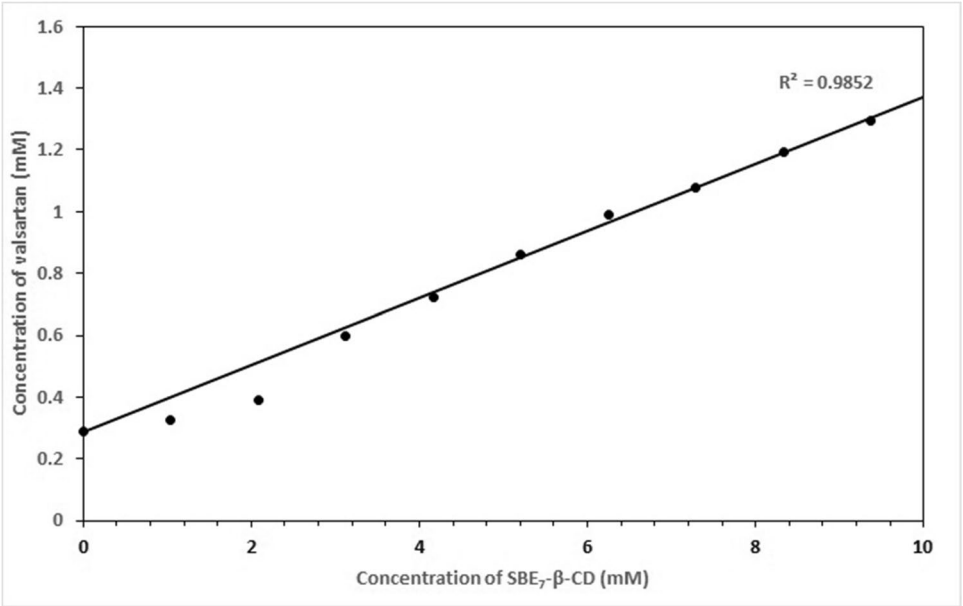

Fig. 1 Phase solubility diagram of valsartan with SBE_7-β-CD

dissolution in an aqueous media [41]. Negative ΔG_{tr}° values suggest that the solubility and dissolution profile has improved, as shown in Table II.

Analysis of Drug Content

The physical mixture and kneading inclusion complex show percentage drug content 98.1 ± 0.81 and 97.12 ± 0.85, respectively ($n = 3$). Stat Ease Design Expert 13 examined the cumulative effect of independent variables on response. Twenty batches of inclusion complexes of valsartan with SBE_7-β-CD were prepared, and it was determined what proportion of the drug was present. The findings are presented in Table III.

Table II Effect of SBE_7-β-CD concentration and Gibbs free energy on solubility of valsartan

S. No	Concentration of SBE_7-β-CD (mM)	Concentration of valsartan (mM)	ΔG (J/M)
1	0	0.28 ± 0.12	0
2	0.5	0.32 ± 0.42	− 300.28
3	1	0.38 ± 0.54	− 753.06
4	1.5	0.59 ± 0.43	− 1817.93
5	2	0.72 ± 0.38	− 2281.13
6	2.5	0.85 ± 0.65	− 2714.82
7	3	0.99 ± 0.45	− 3071.31
8	3.5	1.07 ± 0.44	− 3279.49
9	4	1.19 ± 0.17	− 3532.36
10	4.5	1.29 ± 0.36	− 3731.37
11	5	1.45 ± 0.78	− 4011.33

Table III Experimental matrix of valsartan inclusion complexes using central composite design ($n = 3$)

	Levels of independent variables employed			Valsartan SBE_7-β-CD inclusion complexes
	X_1	X_2	X_3	% Drug Content
Run	A: Power (W)	B: Time (sec)	C: Solvent (ml)	
1	600	10	3	95.8 ± 0.23
2	400	65	2	86.3 ± 0.69
3	400	65	2	85.8 ± 0.85
4	200	65	2	65.4 ± 0.15
5	400	65	2	85.2 ± 0.25
6	600	120	3	90.3 ± 079
7	200	120	1	70.9 ± 0.14
8	400	120	2	98.6 ± 0.36
9	600	65	2	96.9 ± 0.45
10	600	120	1	88.4 ± 0.96
11	400	65	3	90.9 ± 0.52
12	400	65	2	89.4 ± 0.89
13	400	65	1	85.6 ± 0.45
14	200	120	3	75.1 ± 0.96
15	400	65	2	90.3 ± 0.23
16	200	10	1	30.1 ± 0.73
17	400	65	2	90.9 ± 0.29
18	400	10	2	70.4 ± 0.85
19	200	10	3	35.6 ± 0.45
20	600	10	1	90.8 ± 0.69

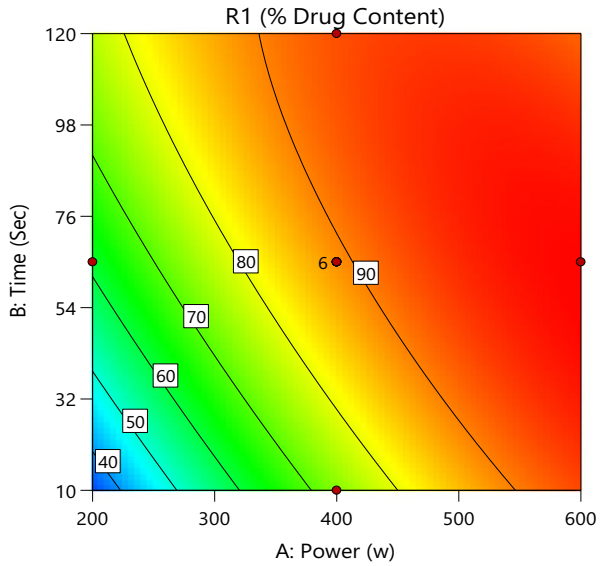
R1 (% Drug Content)
B: Time (Sec)
A: Power (w)
120
98
76
54
32
10
200
300
400
500
600
40
50
60
70
80
90
6

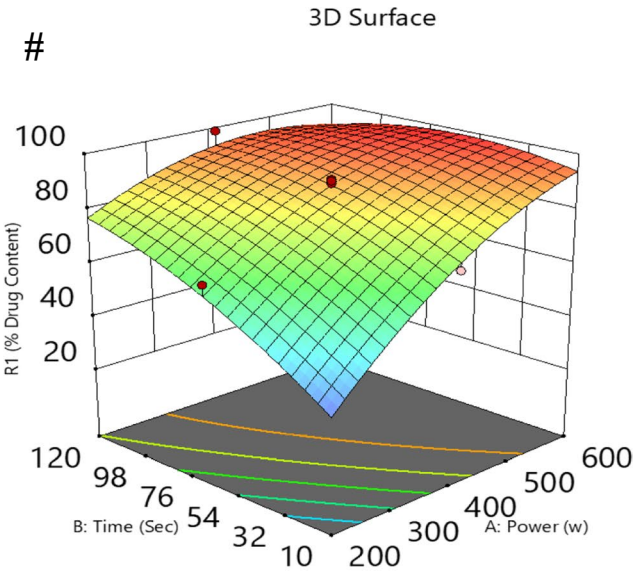
3D Surface
#
R1 (% Drug Content)
B: Time (Sec)
A: Power (w)
100
80
60
40
20
120
98
76
54
32
10
200
300
400
500
600

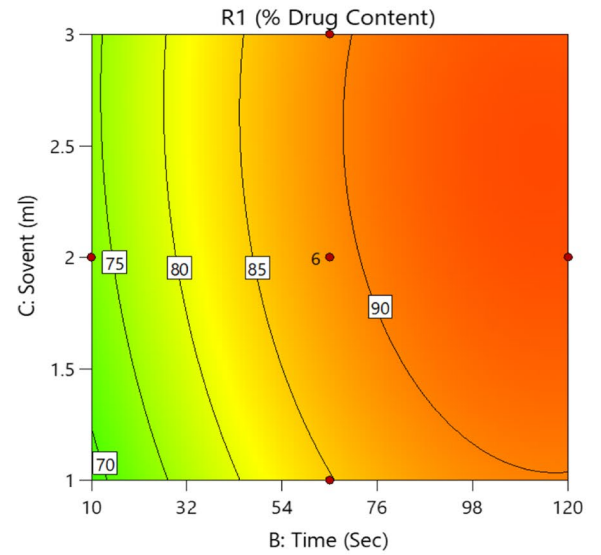
R1 (% Drug Content)
C: Sovent (ml)
B: Time (Sec)
3
2.5
2
1.5
1
10
32
54
76
98
120
70
75
80
85
90
6

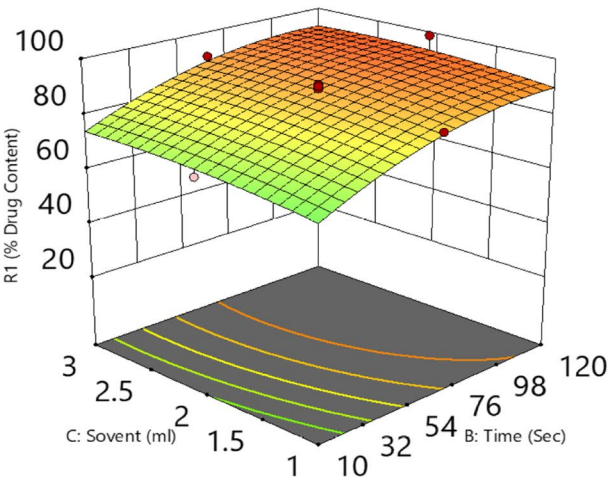
R1 (% Drug Content)
C: Sovent (ml)
B: Time (Sec)
100
80
60
40
20
3
2.5
2
1.5
1
120
98
76
54
32
10

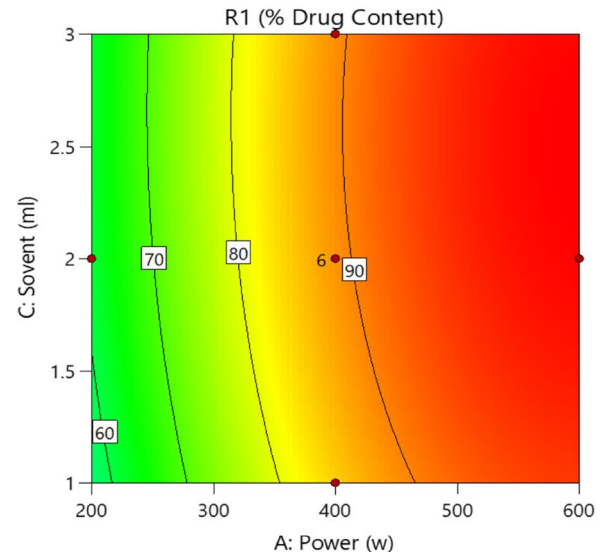
R1 (% Drug Content)
C: Sovent (ml)
A: Power (w)
3
2.5
2
1.5
1
200
300
400
500
600
60
70
80
90
6

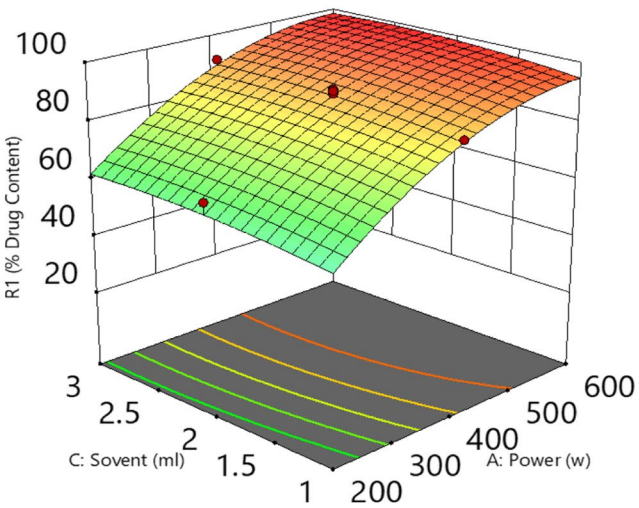
R1 (% Drug Content)
C: Sovent (ml)
A: Power (w)
100
80
60
40
20
3
2.5
2
1.5
1
600
500
400
300
200

◀ **Fig. 2** Contour and three-dimensional response surface plots exhibiting independent variable influence on dependable variable

Optimisation of Process Variables in Microwave-Irradiated Complexes

Preliminary Trials

The smallest amount of power needed for the reaction is 200 W for 10 s with 3 ml of ethanol, and charring is noticed after 300 s. On the other hand, charring happens in 120 s when 800 W is used with 1 ml of solvent. After being irradiated, the samples were dried out in an oven and then analysed to determine the amount of drug they contained.

Experimental Design and Statistical Data Analysis

The valsartan inclusion complexes prepared with SBE_7-β-CD using microwave irradiation show percentage drug concentrations in the range of 30.1 ± 0.73 to 98.6 ± 0.36. Drug content in prepared inclusion complexes was significant ($p < 0.05$) in the quadratic model. Multiple linear regression generated polynomial model equations for all response variables. The polynomial equation relating the percentage drug content for valsartan inclusion complexes prepared with SBE_7-β-CD using microwave irradiation is

$$R_1 = 88.83 + 18.51X_1 + 10.06X_2 + 2.19X_3 - 11.02X_1X_2 - 0.35X_1X_3 - 0.55X_2X_3 - 8.95{X_1}^2 - 5.60{X_2}^2 - 1.85{X_3}^2$$

The coefficient estimates provide the estimated response change per unit change in factor value, while all other factors are maintained constant. The adjusted R^2 of 0.9693 is pretty close to the predicted R^2 of 0.9122. The difference is smaller than 0.2. Accuracy is employed as a measurement for the signal-to-noise ratio. The obtained value is 29.71. From the above model equation, $F = 67.62$ indicates model significance. The terms in the model that have p values less than 0.05 are considered significant. X_1, X_2, X_1X_2, ${X_1}^2$, and ${X_2}^2$ significantly affect the percentage drug content. Due to the fact that the F value for the lack of fit is 2.42 indicates

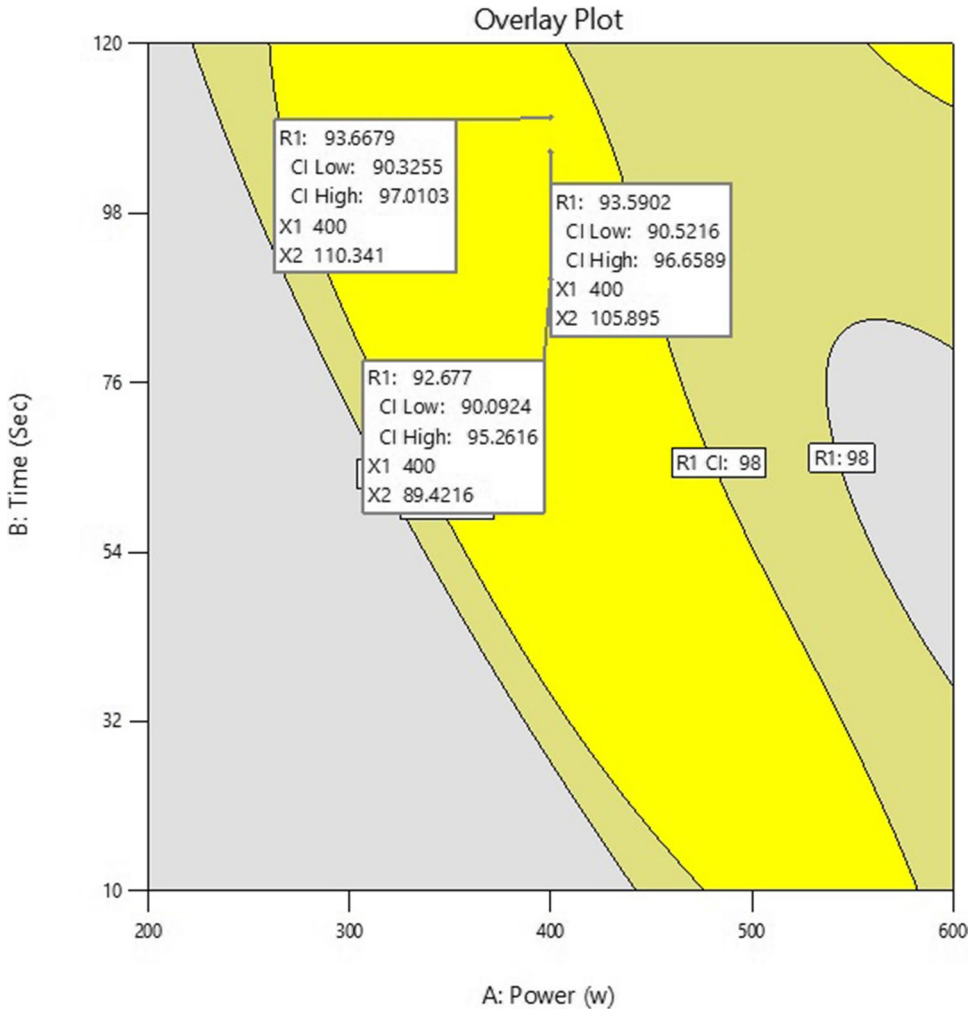

Fig. 3 Graphical optimisation through overlay plots showing the optimal variable settings for model validation

Table IV Optimisation process variables for the preparation of inclusion complexes

Responses	Batch	X_1 Power(W)	X_2 Time (sec)	Observed value (mean ± SD, $n = 3$)	Predicted value	% error
Drug content in SBE_7-β-CD-irradiated inclusion complexes	VSMWC 1	400	110	95.42 ± 0.69	93.66	1.85
	VSMWC 2	400	105	95.84 ± 0.43	93.59	2.4
	VSMWC 3	400	89	93.56 ± 0.74	92.67	0.9

that it is not statistically significant when compared to the pure error. There is a likelihood of 17.74% that a lack of fit F value as high as this one could be the result of noise. We want an accurate model; therefore, a small lack of fit is desirable [42].

A response surface approach was applied in order to learn more about how the combined effects of independent variables affect specified responses. Response surface methodology lets you make plots of response surfaces in three dimensions and plots of contours in two dimensions. Three-dimensional response surface plots help explain the independent variables' main and interaction effects, whereas two-dimensional contour lines show the values of the response, as shown in Fig. 2. The software made contour plots and 3D response plots that helped demonstrate how the data from the twenty experimental runs on each response appeared. When power (X_1), time (X_2), and amount of solvent (X_3) increase, drug content initially increases but then drops due to drug degradation at high power. The results also indicate there is significant interaction between the variables X_1 and X_2, which ultimately affects the output.

Optimisation of Process Variables

After constraining each component and response, the software suggested several independent variable ratios. Three inclusion ratios were chosen to test the model's validation and optimisation abilities. By analysing the desirability function, numerical optimisation was performed; the target was inside the range, and constraints were imposed ($200 \leq X_1$ 600 W target 400 W, $10 \leq X_2 \leq 120$ s, and $1 \leq X_3 \leq 3$ ml). The desirability function of chosen solutions was determined to be 1, showing the model's appropriateness. After applying the constraints for response presented in Fig. 3, a graphical optimisation is performed by building overlay graphs. The characteristics of these three batches suggest that their observed values were close to those anticipated by the programme in Table IV. The observed percentage error is in the range of 0.9 to 1.85, the lowest possible error rates, demonstrating that factorial models reliably predict process variables. The prepared inclusion complex VSMWC 3 was then tested and characterised for dissolution rate.

Evaluation of Prepared Formulations

The precompression parameters of the resulting mixture for each formulation are analysed. and the results are shown in Table V. The results show that the blends were suitable for direct compression. The formulations prepared are evaluated for quality control tests, and the results are shown in Table VI. All values fall within ranges that are suitable for tablet direct compression.

In vitro Drug Release Studies

Studies on *In Vitro* Dissolution Rate of Complexes

Pure drug and all inclusion complex dissolution curves are shown in Fig. 4. Physical combination and kneading inclusion complexes dissolved better than pure drug, according to these findings. The valsartan SBE_7-β-CD inclusion complex (VSMWC 3) demonstrates a greater rate of dissolution compared to the physical mixture and kneading inclusion complex.

A two-way analysis of variance (ANOVA) was used to statistically analyse the % DE_{30min} values for the formulations at $p < 0.05$, which denotes a significant difference. Microwave irradiation of inclusion complexes likely causes solubilisation, amorphisation, and enhanced wettability,

Table V Precompression parameters for various blends of formulations

Formulation	Bulk density (g/ml)	Tapped density (g/ml)	Angle of repose (°)	Compressibility index (%)
F_1	0.53 ± 0.08	0.60 ± 0.15	26.56 ± 0.56	11.66
F_2	0.53 ± 0.11	0.60 ± 0.18	26.13 ± 0.89	11.66
F_3	0.55 ± 0.12	0.62 ± 0.45	25.69 ± 0.98	11.29
F_4	0.55 ± 0.14	0.62 ± 0.39	25.56 ± 0.45	11.29

Table VI Evaluation of prepared formulations

Formulation	Weight variation	Friability (%)	Drug content (%)	Disintegration time (sec)
F_1	301.0 ± 0.62	0.26	99.12 ± 0.5	43 ± 1
F_2	301.5 ± 0.43	0.56	99.23 ± 0.1	38 ± 2
F_3	300.5 ± 0.32	0.21	99.29 ± 0.1	32 ± 1
F_4	299.5 ± 0.69	0.28	99.24 ± 0.4	32 ± 3

all of which contribute to a higher dissolution rate. In both instances, the dissolution rate was enhanced in the ways described below: valsartan < physical mixture < kneading complex < microwave irradiated complex, suggesting that inclusion complex preparation affected dissolution. Microwave-irradiated complex improves the dissolution rate of valsartan by 2.85-fold.

In Vitro Dissolution Study of Formulation

As shown in Fig. 5, *in vitro* dissolution analyses of developed formulations and Diovan® tablet are performed in phosphate buffer pH 6.8. The dissolution rates of formulations F_1 to F_4 demonstrate that the dissolution rate increases as the superdisintegrant concentration increases. The rate and extent of drug dissolution were quantified by determining the dissolution efficiency after 30 min (% DE_{30min}). A two-way analysis of variance (ANOVA) was used to statistically analyse the % DE_{30min} values for the formulations at $p < 0.05$, which denotes a significant difference. Among the formulations, F_3 demonstrates the best dissolving efficiency, i.e., 68.5%. Further calculation of f_1 and f_2 values for F_3 and Diovan® was determined to be within the acceptable range, i.e., 5.68 and 63.94, respectively. Formulation F_3 was characterised and used for *in vivo* bioavailability studies.

Fourier Transform Infrared Spectroscopy

The FTIR spectra of valsartan, inclusion complexes, and the F_3 formulation are shown in the Fig. 6. The valsartan pure drug shows the peak at 3034.01 cm^{-1} linked to O—H stretch, 2960.95 cm^{-1}, 2931.32 cm^{-1}, 2872.22 cm^{-1} linked to C—H stretch, 1733.78 cm^{-1} linked to C = O stretch of acid, a peak at 1605 cm^{-1} linked to amide carbonyl stretching, 1597.93 cm^{-1} linked to N—N bending, 1450.03 cm^{-1} linked to C—OH plane banding, 1409.24 cm^{-1} linked to

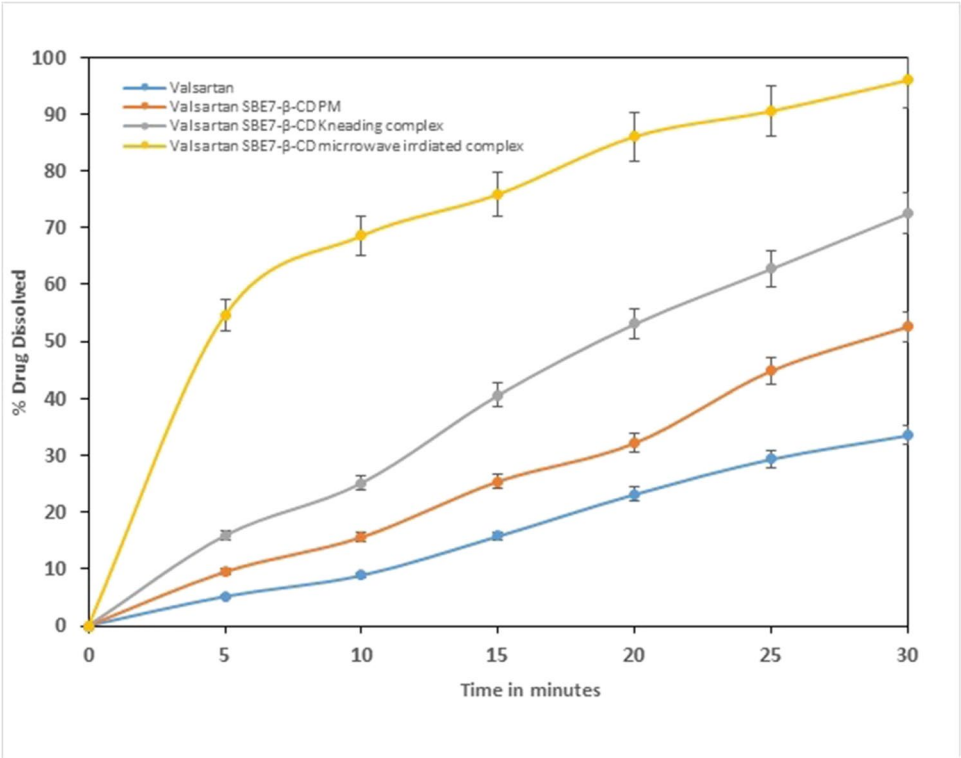

Fig. 4 Drug release from in complexes vs pure valsartan

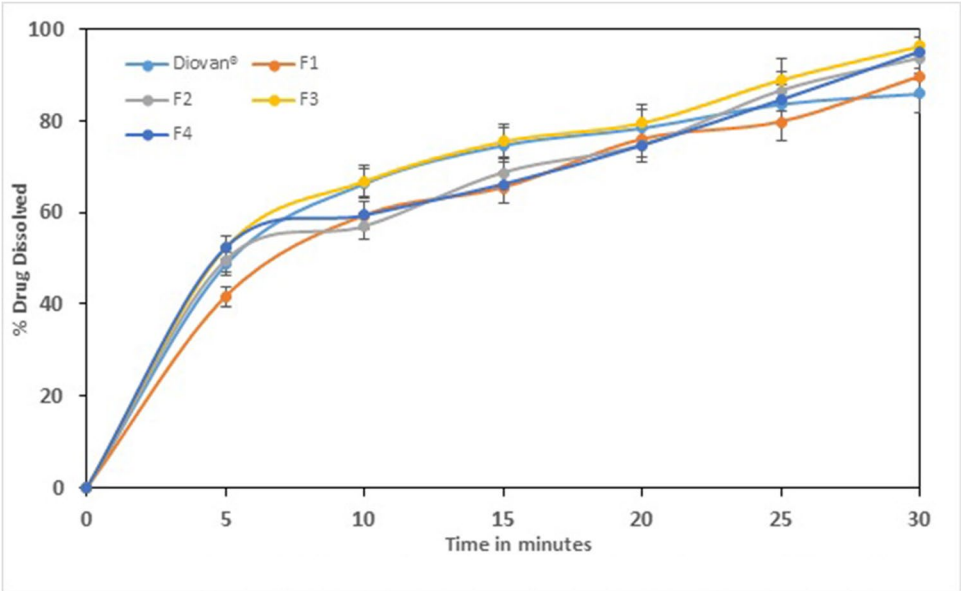

Fig. 5 Drug release from various formulations vs Diovan®

C—O stretching, and 995.52 cm^{-1} linked to C—N stretch and C-H out of plane bending of aromatic ring. In the case of the SBE_7-β-CD, it shows peak at 3390.16 cm^{-1} caused by O—H stretch; the vibrating functional groups of -CH and $-CH_2$ were seen in the 2800–3000 cm^{-1}. The H–O-H stretching was found at an absorption spectrum of 1640.24 cm^{-1}. At 1149.36 cm^{-1}, there is a clear peak caused by the stretching vibration of the C–O–C functional group. A prominent peak at 1029.02 cm^{-1} confirmed the presence of sulfoxide stretching. The results were very similar to those found in a research paper [43]. In the physical mixture, the absorption bands of the pure drug were unaffected. The complexes

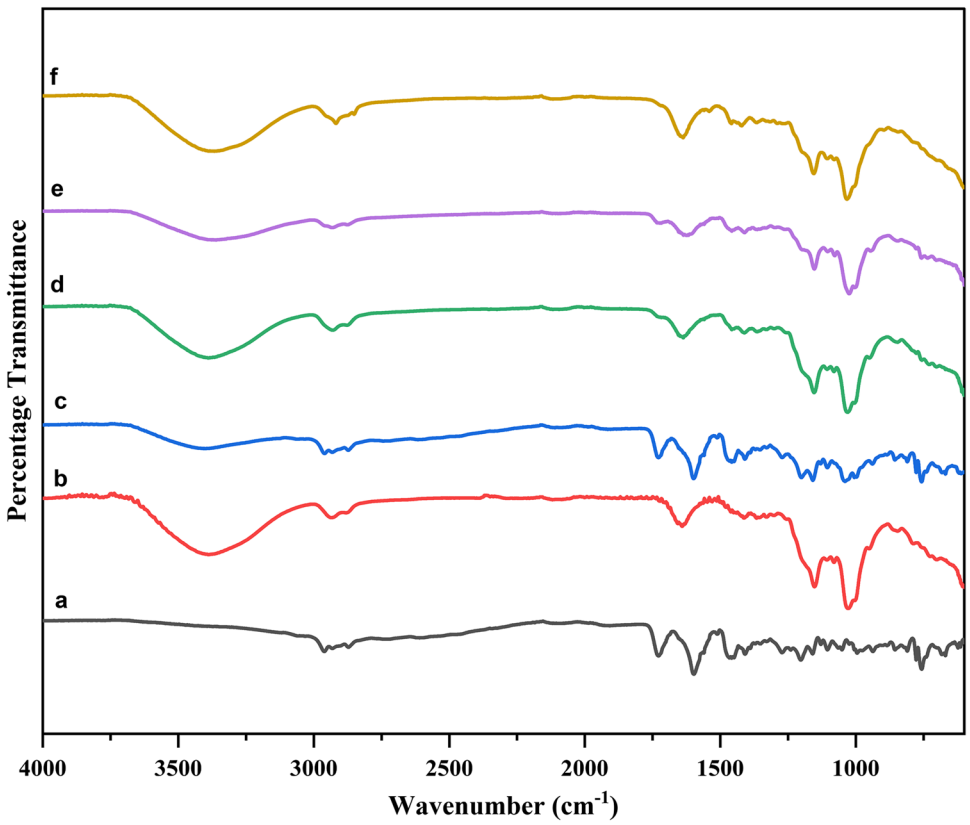

Fig. 6 FTIR spectra of **a** valsartan, **b** SBE_7-β-CD, **c** valsartan SBE_7-β-CD PM, **d** valsartan SBE_7-β-CD kneading complex, **e** valsartan SBE_7-β-CD microwave-irradiated complex, **f** F_3 tablet formulation

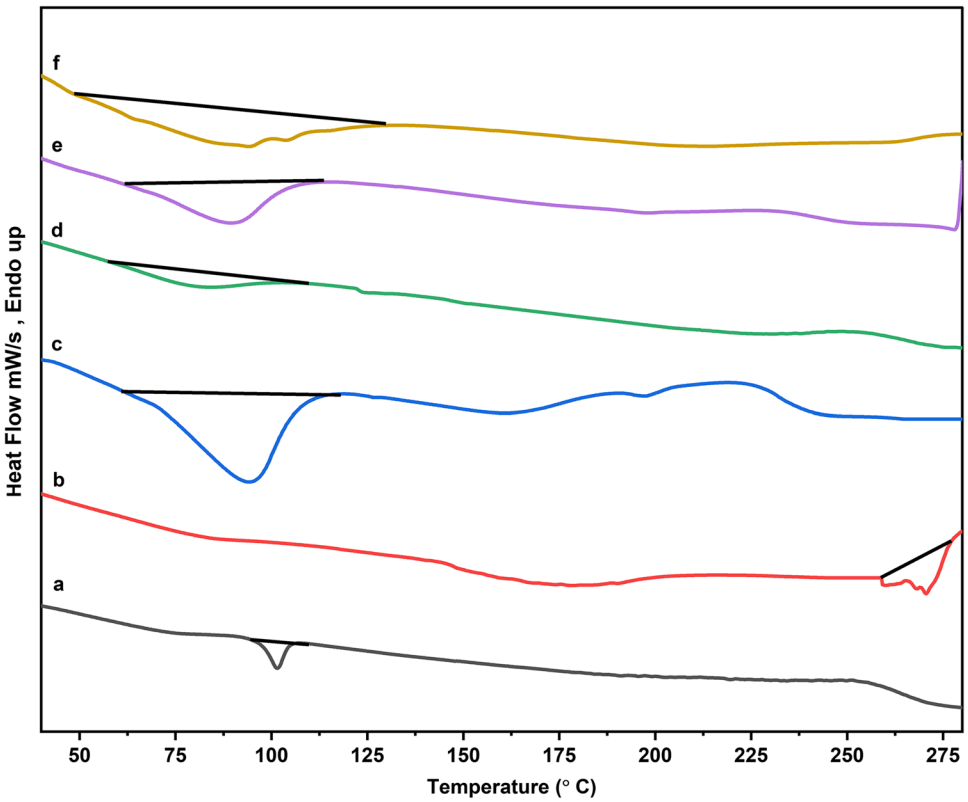

Fig. 7 DSC thermogram of **a** valsartan, **b** SBE_7-β-CD, **c** valsartan SBE_7-β-CD PM, **d** valsartan SBE_7-β-CD kneading complex, **e** valsartan SBE_7-β-CD microwave-irradiated complex, **f** F_3 tablet formulation

and formulation F_3 showed all characteristic peaks of the drug with changes in intensity, and the amide carbonyl band appeared to have been significantly moved to a higher wave number. This behaviour is due to the SBE_7-β-CD interaction with the drug molecule via hydrogen bonds, and the disappearance of C-H bending of the aromatic ring indicates a hindrance caused by a tight fit in the SBE_7-β-CD cavity, thus conforming to inclusion complex formation [44].

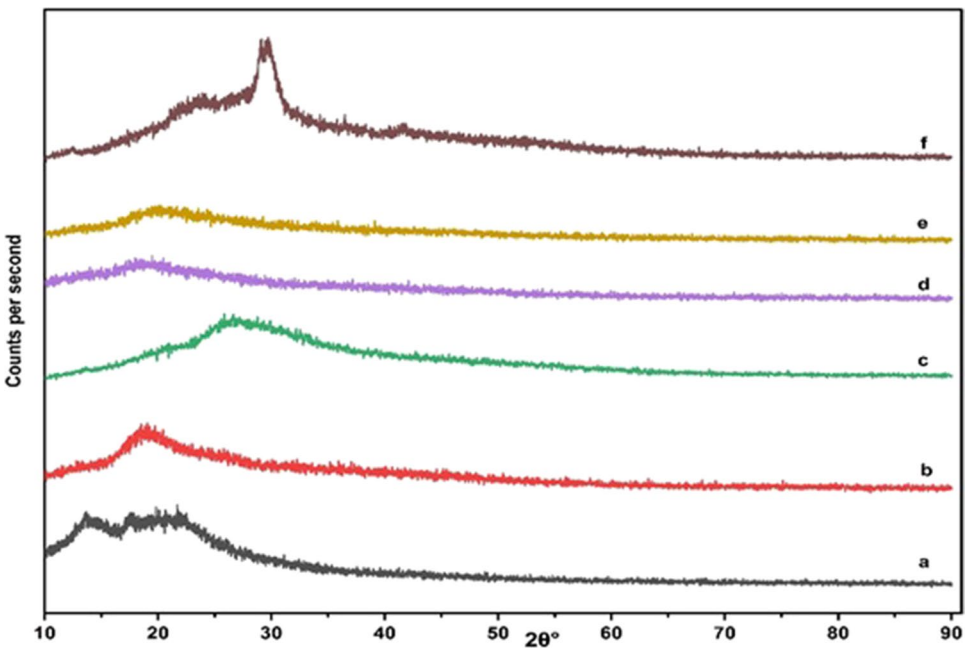

Fig. 8 X-RD plots of **a** valsartan, **b** SBE_7-β-CD, **c** valsartan SBE_7-β-CD PM, **d** valsartan SBE_7-β-CD kneading complex, **e** valsartan SBE_7-β-CD microwave-irradiated complex, **f** F_3 tablet formulation

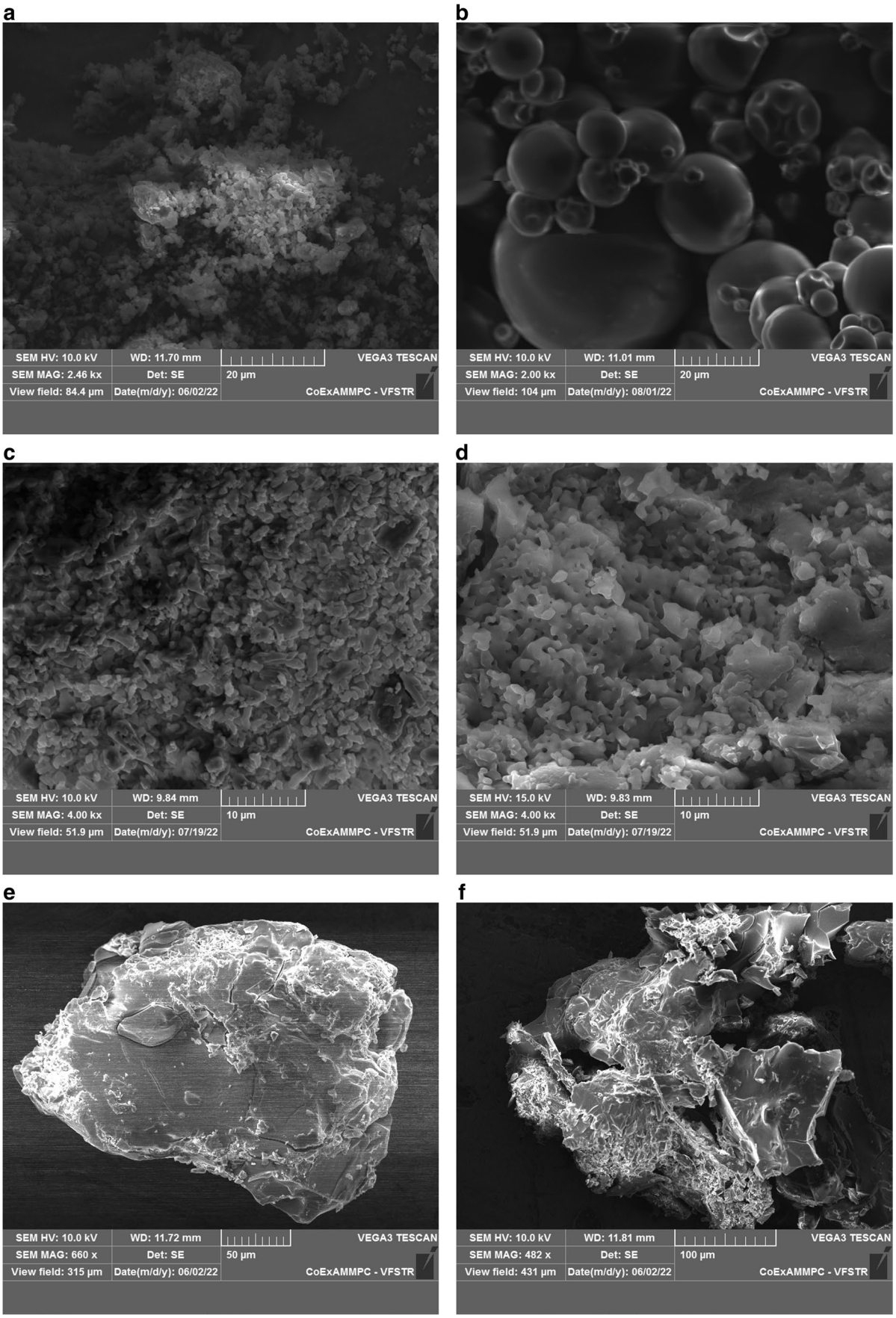
a
SEM HV: 10.0 kV
WD: 11.70 mm
VEGA3 TESCAN
SEM MAG: 2.46 kx
Det: SE
20 µm
View field: 84.4 µm
Date(m/d/y): 06/02/22
CoExAMMPC - VFSTR
b
SEM HV: 10.0 kV
WD: 11.01 mm
VEGA3 TESCAN
SEM MAG: 2.00 kx
Det: SE
20 µm
View field: 104 µm
Date(m/d/y): 08/01/22
CoExAMMPC - VFSTR
c
SEM HV: 10.0 kV
WD: 9.84 mm
VEGA3 TESCAN
SEM MAG: 4.00 kx
Det: SE
10 µm
View field: 51.9 µm
Date(m/d/y): 07/19/22
CoExAMMPC - VFSTR
d
SEM HV: 15.0 kV
WD: 9.83 mm
VEGA3 TESCAN
SEM MAG: 4.00 kx
Det: SE
10 µm
View field: 51.9 µm
Date(m/d/y): 07/19/22
CoExAMMPC - VFSTR
e
SEM HV: 10.0 kV
WD: 11.72 mm
VEGA3 TESCAN
SEM MAG: 660 x
Det: SE
50 µm
View field: 315 µm
Date(m/d/y): 06/02/22
CoExAMMPC - VFSTR
f
SEM HV: 10.0 kV
WD: 11.81 mm
VEGA3 TESCAN
SEM MAG: 482 x
Det: SE
100 µm
View field: 431 µm
Date(m/d/y): 06/02/22
CoExAMMPC - VFSTR

◀ **Fig. 9** SEM images of **a** valsartan, **b** SBE_7-β-CD, **c** valsartan SBE_7-*β*-CD PM, **d** valsartan SBE_7-β-CD kneading complex, **e** valsartan SBE_7-β-CD microwave-irradiated complex, **f** valsartan SBE_7-β-CD microwave-irradiated complex

Thermal Analysis

Figure 7 depicts the DSC studies of valsartan, SBE_7-β-CD, generated complexes, and F_3 formulation, done to look into solid-state interactions and how the manufacturing process affects them. The melting point of valsartan was shown on the thermogram as an endothermic peak at 101.5 °C. Beginning at 258 °C and rising to 272 °C, the thermograph of SBE_7-β-CD revealed a large endothermic peak associated with bound water loss. The physical mixture of valsartan and SBE_7-β-CD exhibits a wide peak between 60 °C and 115 °C. The kneading complex exhibited a broad endothermic peak beginning at 56 °C and ending at 103.6 °C, whereas the microwave-irradiated complex exhibited a broad endothermic peak beginning at 60 °C and ending at 110 °C. In both instances, the drug's typical peak intensity decreased and vanished, indicating the creation of an amorphous inclusion complex. In the case of F_3 formulation, a wide endothermic peak from 49 to 128 °C is seen. The complete disappearance of the crystalline drug melting peak in the DSC curve of the supposed complex is commonly taken as proof of drug molecule entry into the CD cavity.

Powder X-Ray Diffraction

Samples are examined for valsartan crystalline states with X-ray diffraction studies as shown in Fig. 8. The valsartan developed inclusion complexes, and the valsartan tablet samples displayed amorphous characteristics. The valsartan exhibited crystalline peaks (2°θ) at 10.74°, 11.7°, 12.82°, 13.68°, 15.16°, 17.64°, 18.28°, 19.82°, 21.68°, 23.2°, 26.04°, and 30.62°. The complex treated with microwaves had intensified crystalline peaks at 11.54°, 12.15°, 12.62°, 13.08°, 13.54°, 13.92°, 14.62°, 15.24°, 16.62°, 17.91°, 18.38°, 18.8°, 19.12°, 19.67°, 20.13°, 21.53°, 22.40°, 23.28°, 25.27°, 27.95°, 30.64°, and 35.40°. The degree of crystallinity of valsartan was determined to be 63.02%, whereas that of the microwave-irradiated complex was 44.53%. The degree of crystallinity of the inclusion complex produced by microwave irradiation exhibited a substantial shift. After microwave irradiation, the results indicated that the crystalline character of valsartan in the produced inclusion complex was significantly diminished. The degree of crystallinity of the tablet formulation produced with microwave irradiation is 55.80%, with distinctive peaks (2°θ) at 10.97°, 11.87°,

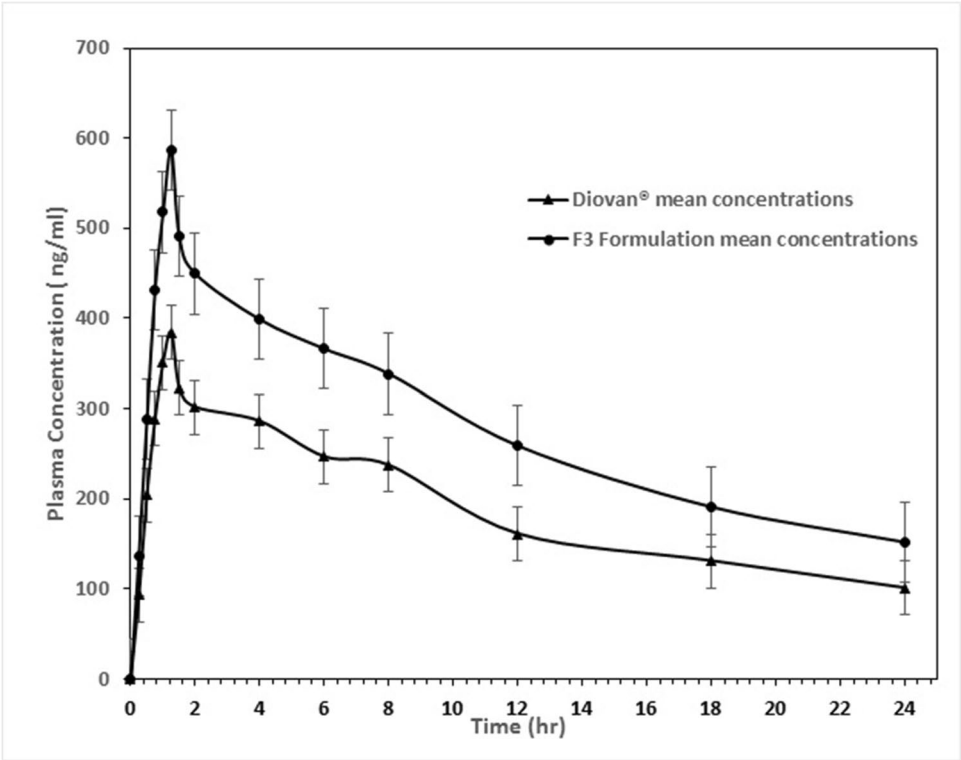

Fig. 10 Plasma concentration time profiles of valsartan after oral administration of Diovan® and F_3 tablet formulation

Table VII Pharmacokinetic parameters of valsartan after rat oral administration

Pharmacokinetic parameter	Each value represents the mean ± SD ($n=6$)	
	Diovan®	F_3 formulation
C_{max} (ng/ml)	380.93 ± 3.8	586.43 ± 2.65
T_{max} (h)	1.25 ± 0.00	1.25 ± 0.00
$AUC_{0\text{-}24}$ (h. ng/ ml)	4494.38 ± 32.47	6665.34 ± 28.36
$AUC_{0\text{-}\infty}$ (h. ng/ ml)	6841.67 ± 16.52	9687.79 ± 12.36
$t_{1/2}$ (h)	6.36 ± 0.56	6.45 ± 0.49

12.44°, 14.91°, 15.62°, 16.91°, 17.92°, 19.63°, 22.08°, 22.64°, 22.89°, 25.26°, 26.32°, 28.77°, 29.50°, 30.27°, and 34.80°. New diffractive peaks in the inclusion complex spectra, the shift of drug molecule distinctive peaks, and changes in their relative intensities indicate the emergence of a new solid phase, which supports inclusion complex formation.

Scanning Electron Microscopy Studies

Figure 9 presents the results of scanning electron microscopy findings on the shape and particle size of valsartan, SBE_7-β-CD, the kneading complex, and the microwave-irradiated complex. Crystals with an amorphous appearance like valsartan were found. The SEM micrograph of SBE_7-β-CD revealed spherical particles. After going through the process of inclusion complexation, SBE_7-β-CD became less spherical, had a smooth surface, and contained smaller particles. Within the inclusion complexes, it was noticed that the drug particle morphology changed significantly. A possible interaction between the valsartan and the SBE_7-β-CD was indicated by the fact that it was impossible to separate the drug from the SBE_7-β-CD.

Pharmacokinetic Study

After oral administration to rats, the pharmacokinetic parameters of valsartan in commercial formulation and F_3 formulation were examined. Figure 10 depicts the mean plasma concentration of valsartan *vs.* time profile in rats. The plasma concentrations of valsartan in the F_3 formulation were found to be significantly greater than those seen in the product that is already on the market. Particularly, when compared to the commercial formulation, the F_3 formulation produced higher initial plasma concentrations due to the formulation's faster rate of dissolution. The non-compartmental approach is used to figure out the pharmacokinetic parameters, which are shown in Table VII. A two-way ANOVA performed between groups revealed a significant difference in C_{max}, $AUC_{0\text{-}24}$, and $AUC_{0\text{-}\infty}$ values at $p<0.05$. The F_3 formulation shows a significantly higher C_{max}, $AUC_{0\text{-}24}$, and $AUC_{0\text{-}\infty}$ of valsartan compared to the Diovan® ($p<0.05$). The obtained values were close to those reported in early published article [45]. The AUC of the F_3 formulation was about 1.4-fold higher than Diovan®. However, the $t_{1/2}$ values of the valsartan in both formulations did not significantly differ. Thus, the F_3 formulation's higher dissolving rate may increase valsartan absorption in rats, increasing oral bioavailability.

Conclusion

In this study, adding modified cyclodextrin like SBE_7-β-CD made valsartan more soluble because of electronic interactions. The phase solubility experiments reveal A_L-type curves; hence, inclusion complexes were prepared using an equal molar ratio. The values of Gibbs free energy (ΔG_{tr}°) associated with the water solubility of valsartan in the presence of cyclodextrin were all negative and declined with increasing concentration, demonstrating the spontaneous nature of drug solubilisation. Valsartan inclusion complexes were produced using the kneading and microwave irradiation techniques. The process variables in microwave irradiation technique for preparing valsartan and SBE_7-β-CD inclusion complexes were optimised using a central composite face design. The prepared inclusion complexes were further used for dissolution rate testing and characterisation. The valsartan inclusion complexes with SBE_7-β-CD microwave irradiation technique (VSMWC 3) showed 2.85-fold enhanced dissolution rate compared with pure valsartan. The DSC thermographs of microwave-irradiated complexes indicated solid-state interaction, and X-ray diffraction revealed the amorphisation of valsartan in the complexes. The FTIR spectra indicate no significant change in the characteristic peaks of functional groups. The SEM images for VSMWC 3 revealed drastic changes in the structure of the inclusion complexes, namely, the morphology and form of the drug particles. The inclusion complex VSMWC 3 was formulated into various tablet dosage forms (F_1 to F_4) by adding inactive ingredients using the direct compression technique. The tablet formulation F_3 was tested in rats for bioavailability based on *in vitro* drug release and the similarity factor (f_2) to Diovan®. The *in vivo* results demonstrate an increase in C_{max} and AUC for the tablet formulation F_3 compared to Diovan®, thus enhancing valsartan oral bioavailability.

Acknowledgements The author acknowledges the assistance of Centre of Excellence (CoExAMMPC)—VFSTR at Vignan's Foundation for Science, Technology, & Research in characterising the samples.

Author Contribution Author 1: The work's design, analysis, and interpretation of data.

Author 2: Guidance and drafting the work

Declarations

Conflict of Interest The authors declare no competing interests.

References

1. Cappello B, Maio CD, Iervolino M, Miro A. Improvement of solubility and stability of valsartan by hydroxypropyl-beta-cyclodextrin. J Incl Phenom Macrocycl Chem. 2005;54(3–4):289–94. https://doi.org/10.1007/s10847-005-9004-y.
2. Siddiqui N, Husain A, Chaudhry L, Alam MS, Mitra M, Bhasin PS. Pharmacological and pharmaceutical profile of valsartan: a review. J Appl Pharm Sci. 2011;01(04):12–9.
3. Beg S, Swain S, Singh HP, Patra ChN, Rao ME. Development, optimization, and characterization of solid self-nanoemulsifying drug delivery systems of valsartan using porous carriers. AAPS PharmSciTech. 2012;13(4):1416–27. https://doi.org/10.1208/s12249-012-9865-5.
4. Cao QR, Liu Y, Xu WJ, Lee BJ, Yang M, Cui JH. Enhanced oral bioavailability of novel mucoadhesive pellets containing valsartan prepared by a dry powder-coating technique. Int J Pharm. 2012;434(1–2):325–33. https://doi.org/10.1016/j.ijpharm.2012.05.076.
5. Nasr AM, Moftah F, Abourehab MAS, Gad S. Design, formulation, and characterization of valsartan nanoethosomes for improving their bioavailability. Pharmaceutics. 2022;14:2268. https://doi.org/10.3390/pharmaceutics14112268.
6. Meruva S, Thool P, Shah S, Karki S, Bowen W, Ghosh I, et al. Formulation and performance of Irbesartan nanocrystalline suspension and granulated or bead-layered dried powders - Part I. Int J Pharm. 2019;568:118189. https://doi.org/10.1016/j.ijpharm.2019.03.007.
7. Koseki N, Kawashita H, Hara H, Niina M, Tanaka M, Kawai R, et al. Development and validation of a method for quantitative determination of valsartan in human plasma by liquid chromatography-tandem mass spectrometry. J Pharm Biomed Anal. 2007;43(5):1769–74. https://doi.org/10.1016/j.jpba.2006.12.030.
8. Enggi CK, Satria MT, Nirmayanti N, Usman JT, Nur JF, Asri RM, et al. Improved transdermal delivery of valsartan using combinatorial approach of polymeric transdermal hydrogels and solid microneedles: an ex vivo proof of concept investigation. J Biomater Sci Polym Ed. 2022;34:(3)334–350. https://doi.org/10.1080/09205063.2022.2121590.
9. Sakai K, Sato Y, Okada M, Yamaguchi S. Cyclodextrins produced by cyclodextrin glucanotransferase mask beany off-flavors in plant-based meat analogs. PLOS ONE. 2022;17:e0269278. https://doi.org/10.1371/journal.pone.0269278.
10. Challa R, Ahuja A, Ali J, Khar RK. Cyclodextrins in drug delivery: an updated review. AAPS PharmSciTech. 2005;6:E329–57. https://doi.org/10.1208/pt060243.
11. Fang S, Peng X, Liang X, Shen J, Wang J, Chen J, et al. Enhancing water solubility and stability of natamycin by molecular encapsulation in methyl-β-cyclodextrin and its mechanisms by molecular dynamics simulations. Food Biophys. 2019;15(2):188–95. https://doi.org/10.1007/s11483-019-09620-z.
12. Yan VC, Muller FL. Captisol and GS-704277, but not GS-441524, are credible mediators of remdesivir's nephrotoxicity. Antimicrob Agents Chemother. 2020;64(12):e01920–20. https://doi.org/10.1128/AAC.01920-20.
13. Rabbani NR, Seville PC. The influence of formulation components on the aerosolisation properties of spray-dried powders. J Control Release. 2005;110(1):130–40. https://doi.org/10.1016/j.jconrel.2005.09.004.
14. Ratti C. Hot air and freeze-drying of high-value foods: a review. 2001;49:311–319. hhttps://doi.org/10.1016/S0260-8774(00)00228-4.
15. Mohit V, Harshal G, Neha D, Vilasrao K, Rajashree H. A comparative study of complexation methods for cefdinir-hydroxypropyl-β-cyclodextrin system. J Incl Phenom Macrocycl Chem. 2010;71(1–2):57–66. https://doi.org/10.1007/s10847-010-9901-6.
16. Gulmezoglu E, Yildiz Turkyilmaz G, Karasulu HY. Preparation and evaluation of a lipid-based drug delivery system to improve valsartan oral bioavailability: pharmacokinetic and pharmacodynamic analysis. Drug Dev Ind Pharm. 2022;48(12):727–36. https://doi.org/10.1080/03639045.2022.2164588.
17. Shin D, Chae B, Goo Y, Yoon H, Kim C, Sohn S, et al. Improved dissolution and oral bioavailability of valsartan using a solidified supersaturable self-microemulsifying drug delivery system containing gelucire® 44/14. Pharmaceutics. 2019;11:58. Available from: https://doi.org/10.3390/pharmaceutics11020058.
18. Jensen CE, dos Santos RA, Denadai AM, Santos CF, Braga AN, Sinisterra RD. Pharmaceutical composition of valsartan: beta-cyclodextrin: physico-chemical characterization and anti-hypertensive evaluation. Molecules. 2010;15(6):4067–84. https://doi.org/10.3390/molecules15064067.
19. Higuchi T, Connors KA. Phase solubility techniques. Adv Anal Chem Instrum. 1965;4:117.
20. Ranpise NS, Kulkarni NS, Mair PD, Ranade AN. Improvement of water solubility and in vitro dissolution rate of aceclofenac by complexation with beta-cyclodextrin and hydroxypropyl-beta-cyclodextrin. Pharm Dev Technol. 2010;15(1):64–70. https://doi.org/10.3109/10837450903002165.
21. Ghosh A, Biswas S, Ghosh T. Preparation and evaluation of silymarin beta-cyclodextrin molecular inclusion complexes. J Young Pharm. 2011;3(3):205–10. https://doi.org/10.4103/0975-1483.83759.
22. Moneghini M, Bellich B, Baxa P, Princivalle F. Microwave generated solid dispersions containing Ibuprofen. Int J Pharm. 2008;361(1–2):125–30. https://doi.org/10.1016/j.ijpharm.2008.05.026.
23. Cirri M, Maestrelli F, Mennini N, Mura P. Physical-chemical characterization of binary and ternary systems of ketoprofen with cyclodextrins and phospholipids. J Pharm Biomed Anal. 2009;50(5):683–9. https://doi.org/10.1016/j.jpba.2008.11.003.
24. Ryno LM, Levine Y, Iovine PM. Synthesis, characterization, and comparative analysis of amylose-guest complexes prepared by microwave irradiation. Carbohydr Res. 2014;383:82–8. https://doi.org/10.1016/j.carres.2013.11.010.
25. Wang J, Jiang X, Guo Z, Zheng B, Zhang Y. Insights into the multi-scale structural properties and digestibility of lotus seed starch-chlorogenic acid complexes prepared by microwave irradiation. Food Chem. 2021;361:130171. https://doi.org/10.1016/j.foodchem.2021.130171.
26. Das S, Mohanty S, Maharana J, Jena SR, Nayak J, Subuddhi U. Microwave-assisted β-cyclodextrin/chrysin inclusion complexation: an economical and green strategy for enhanced hemocompatibility and chemosensitivity in vitro. J Mol Liq. 2020;310:113257. https://doi.org/10.1016/j.molliq.2020.113257.
27. Valente JFA, Dias JR, Sousa A, Alves N. Composite central face design-an approach to achieve efficient alginate microcarriers. Polymers (Basel). 2019;11:1949. https://doi.org/10.3390/polym11121949.
28. Godbole MD, Sabale PM, Mathur VB. Development of lamivudine liposomes by three-level factorial design approach for optimum entrapment and enhancing tissue targeting. J Microencapsul. 2020;37(6):431–44. https://doi.org/10.1080/02652048.2020.1778806.

29. Ahmad N, Ahmad R, Al-Qudaihi A, Alaseel SE, Fita IZ, Khalid MS, et al. Preparation of a novel curcumin nanoemulsion by ultrasonication and its comparative effects in wound healing and the treatment of inflammation. RSC Adv. 2019;9(35):20192–206. https://doi.org/10.1039/c9ra03102b.
30. Xu WJ, Xie HJ, Cao QR, Shi LL, Cao Y, Zhu XY, et al. Enhanced dissolution and oral bioavailability of valsartan solid dispersions prepared by a freeze-drying technique using hydrophilic polymers. Drug Deliv. 2016;23(1):41–8. https://doi.org/10.3109/10717544.2014.903012.
31. Zaid A, Qaddomi A, Ghanem M, Shehadeh L, Abualhasan M, Natur S, et al. Development of a dissolution method to compare tablet formulations containing valsartan/amlodipine. Dissolut Technol. 2015;22(3):32–8. https://doi.org/10.14227/dt220315p32.
32. Vranić E, Mehmedagić A, Hadžović S. Mathematical methods for quantification and comparison of dissolution testing data. Biomol Biomed [Internet]. [cited 2023Apr.27] 2002;2(1–2):49–52. Available from: https://www.bjbms.org/ojs/index.php/bjbms/article/view/3581.
33. Husseiny RA, Abu Lila AS, Abdallah MH, El-ghamry HA. Fast disintegrating tablet of Valsartan for the treatment of pediatric hypertension: in vitro and in vivo evaluation. J Drug Deliv Sci Technol. 2018;43:194–200. https://doi.org/10.1016/j.jddst.2017.10.014.
34. Smith B. Infrared spectral interpretation. 2018. https://doi.org/10.1201/9780203750841.
35. Yihong Qiu YC, Geoff G.Z. Zhang, Lawrence Yu, Rao V. Mantri. Developing solid oral dosage forms_ pharmaceutical theory and practice. Academic Press 2016. https://doi.org/10.1016/B978-0-12-802447-8.00002-9.
36. Doumeng M, Makhlouf L, Berthet F, Marsan O, Delbé K, Denape J, et al. A comparative study of the crystallinity of polyetheretherketone by using density, DSC, XRD, and Raman spectroscopy techniques. Polym Test. 2021;93:106878. https://doi.org/10.1016/j.polymertesting.2020.106878.
37. Ni C. Scanning Electron Microscopy (SEM). In: Wang QJ, Chung Y-W, editors. Encyclopedia of Tribology. Boston, MA: Springer, US; 2013. p. 2977–82.
38. Bandopadhyay S, Beg S, Katare OP, Sharma T, Singh B. Integrated Analytical quality by design (AQBD) approach for the development and validation of bioanalytical liquid chromatography method for estimation of valsartan. J Chromatogr Sci. 2020;58(7):606–21. https://doi.org/10.1093/chromsci/bmaa024.
39. Nair AB, Jacob S. A simple practice guide for dose conversion between animals and human. J Basic Clin Pharm. 2016;7(2):27–31. https://doi.org/10.4103/0976-0105.177703.
40. Zhang Y, Huo M, Zhou J, Xie S. PKSolver: An add-in program for pharmacokinetic and pharmacodynamic data analysis in Microsoft Excel. Comput Methods Programs Biomed. 2010;99(3):306–14. https://doi.org/10.1016/j.cmpb.2010.01.007.
41. Biswal S, Sahoo J, Murthy PN, Giradkar RP, Avari JG. Enhancement of dissolution rate of gliclazide using solid dispersions with polyethylene glycol 6000. AAPS PharmSciTech. 2008;9(2):563–70. https://doi.org/10.1208/s12249-008-9079-z.
42. Gelman A. Analysis of variance—why it is more important than ever. Ann Statist. 2005;33(1):1–53. https://doi.org/10.1214/009053604000001048.
43. Alvi Z, Akhtar M, Mahmood A, Ur-Rahman N, Nazir I, Sadaquat H, et al. Enhanced oral bioavailability of epalrestat SBE_7-beta-CD complex loaded chitosan nanoparticles: preparation, characterization and in-vivo pharmacokinetic evaluation. Int J Nanomedicine. 2021;16:8353–73. https://doi.org/10.2147/IJN.S339857.
44. Buchi N. Nalluri RKM, Rao TP, Peter A. Crooks. Effect of recrystallization on the pharmaceutical properties of valsartan for improved therapeutic efficacy. J Appl Pharm Sci. 2012;2(10):126–132. https://doi.org/10.7324/japs.2012.21025.
45. Yan YD, Sung JH, Kim KK, Kim DW, Kim JO, Lee BJ, et al. Novel valsartan-loaded solid dispersion with enhanced bioavailability and no crystalline changes. Int J Pharm. 2012;422(1–2):202–10. https://doi.org/10.1016/j.ijpharm.2011.10.053.